Capillary Interactions Between Anisotropic Colloidal Particles

J. C. Loudet,[1] A. M. Alsayed,[2] J. Zhang,[2] and A. G. Yodh[2]

[1]*Centre de Recherche Paul Pascal, Avenue A. Schweitzer 33600 Pessac, France*

[2]*Department of Physics and Astronomy, University of Pennsylvania, Philadelphia, PA 19104, USA*

(Received 30 July 2004; published 3 January 2005)

We report on the behavior of micron-sized prolate ellipsoids trapped at an oil-water interface. The particles experience strong, anisotropic, and long-ranged attractive capillary interactions which greatly exceed the thermal energy k_BT. Depending on surface chemistry, the particles aggregate into open structures or chains. Using video microscopy, we extract the pair interaction potential between ellipsoids and show it exhibits a power law behavior over the length scales probed. Our observations can be explained using recent calculations, if we describe the interfacial ellipsoids as capillary quadrupoles.

DOI: 10.1103/PhysRevLett.94.018301 PACS numbers: 82.70.Dd, 68.03.Cd, 68.05.Cf

The behavior of particle monolayers at fluid interfaces has attracted interest for many years and across many scientific communities. From a practical viewpoint, the stability of thin liquid films and interfaces in the presence of particles affects the control of a variety of materials including emulsions, foams, and coatings [1]. On the basic science side, particle monolayers form beautiful model systems for studies of fundamental issues in condensed matter physics [2–4]. Nevertheless, questions remain about the mechanism of particle interaction at a fluid interface and about how these interactions lead to formation of ordered and disordered structures.

Perhaps the most important interparticle interaction arising at a fluid interface is due to lateral capillary forces [5,6]. For heavy particles, these capillary interactions stem from the overlap of interface deformations brought about by gravity. Surprisingly, lateral capillary forces also arise for lighter, micron-sized particles. In this case, interfacial deformations can be of electric origin [7,8] or can arise from irregular wetting at the particle surface [6,9–11]. Deformation-driven effects are not the only source of interfacial interactions, however. Interfacially trapped particles have also been observed to experience strong, long-ranged electrostatic repulsions and the competition between these different forces can lead to the formation of well-ordered monolayers with large crystalline areas [12–14].

With a few notable exceptions [15,16], most experimental investigations of interparticle interactions and assembly at fluid-fluid interfaces have focused on spherical or nearly spherical particles. Here, we explore the behavior of anisotropic particles, ellipsoids, at the oil-water interface. Direct measurements of attractive capillary interactions between the ellipsoids are reported. The interaction energies are very large compared to k_BT and compared to the interaction energies of spherical particles with the same surface chemistry. In addition, the pair interaction potential exhibits a power law behavior, which suggests a description in terms of capillary quadrupoles. These anisotropic capillary forces lead to the assembly of open structures and chains rather than crystals or random aggregates.

The anisotropic particles, prolate ellipsoids, were obtained from monodisperse polystyrene (PS) spheres (diameter 4 m, Interfacial Dynamics Corp., USA) following the methods of [17]. Some of the PS ellipsoids were further coated with a silica shell (40–50 nm) using a recently published procedure [18]. We will hereafter refer to these particles as Si ellipsoids. The typical long and short axes of the ellipsoids ranged from 10 to 14 and 1.5 to 2.5 m, respectively. Next, a solution of water and isopropanol (IPA) (1:1 vol.) containing the ellipsoids were spread at the interface between pure water and a mixture of decane (70.5% vol.) and undecane (29.5% vol.) in a small cylindrical glass cell. The composition of the oil phase was chosen in order to match its viscosity to water [13], and the cell walls were made hydrophobic [19]. A flat oil-water interface was thus produced.

Immediately after the turbulent spreading process, a non-negligible interfacial flow was observed. This inevitable initial convection died off within a few tens of seconds. Ellipsoids at the oil-water interface were attracted to one another. These attractions appeared to be long-ranged, extending over distances several times the ellipsoid long axis. The ellipsoid trajectories were very straight. Only very weak angular and positional fluctuations were observed, and the particles stuck irreversibly upon contact. The morphology of the aggregated structures was found to depend on particle surface chemistry. Si ellipsoids aligned preferentially side to side [Fig. 1(a)] while the PS ellipsoids aligned preferentially tip to tip [Fig. 1(b)]. These observations can be explained by the different wetting properties of the particles, which in turn are controlled by their surface chemical compositions. Preferential positioning within the aggregates will tend to minimize the interfacial distortions and thus the overall interfacial energy. In both cases, open branched structures and anisotropic aggregates such as chains were observed [Fig. 1(b) and inset], thus revealing the existence of anisotropic interactions. Slight variations in the ellipsoid aspect ratio, k, between 2.4 and 4.5 did not produce noticeable differences in the structures formed. In addition, we often observed that, once attached, single ellipsoids or packs of

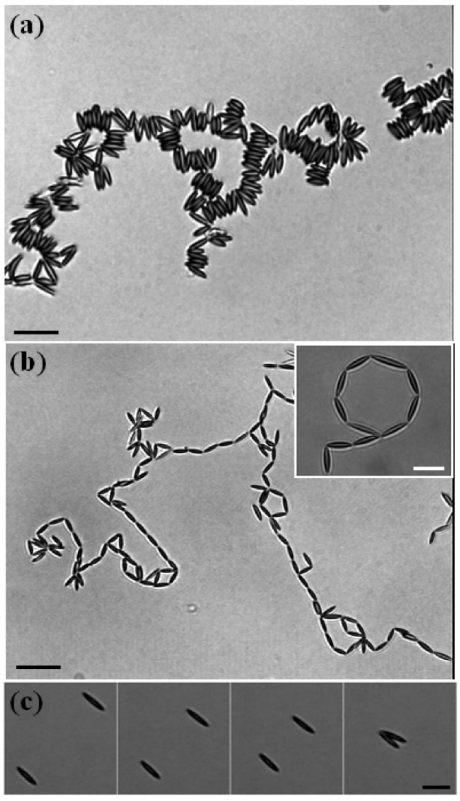

FIG. 1. Optical microscopy pictures of ellipsoidal particles trapped at the water-oil interface. (a) Si ellipsoids aggregate side to side (scale bar: 21 μm), while PS ellipsoids (b) bind in a tip-to-tip manner (scale bar: 33 μm). Inset: polygonlike structure formed by PS ellipsoids (scale bar: 13.6 μm). (c) Typical series of images of two ellipsoids approaching side to side ($k = 4.2$; scale bar: 14 μm).

ellipsoids could freely rotate around one another without coming apart. Evidently, these aggregates are kinetically frozen structures with binding energies larger than k_BT.

Our observations cannot be explained by attractive van der Waals interactions since they are much smaller than k_BT at distances larger than 1 μm [20]. Electrostatic effects due to charged chemical groups bound to the particle surfaces are typically repulsive, and repulsion is observed only at contact. Interestingly, theoretical work predicts [9,10] that even tiny interfacial undulations of a few tens of nanometers are sufficient to yield long-ranged capillary interactions greater than $1000k_BT$. The occurrence of such interactions is extremely likely in our experiments, and this will be further confirmed below.

The ellipsoid behavior described above was in marked contrast with that of spheres with the same surface chemistry. In the latter case, the interaction energies seemed to be comparable to k_BT. The trajectories were very chaotic and the spheres could approach one another very closely without contacting, and then separate again. We suspect these differences between spheres and ellipsoids to be due, at least partly, to the shape anisotropy of the ellipsoids which may produce more complex interfacial distortions and therefore lead to stronger capillary interactions.

In order to better understand these observations, we used optical microscopy to directly measure interactions between the ellipsoids. Working with dilute suspensions, we tracked the motion of pairs of interacting ellipsoids far from other particles. A typical series of images of two ellipsoids approaching side to side is shown in Fig. 1(c). From the recorded videotapes, the approach sequences were digitized, and the particle positions and orientations determined with standard particle tracking routines [21]. From these data the center-to-center separation, r, between two ellipsoids was plotted as a function of time, t (see Fig. 2). The measured attractions are remarkably long ranged; particles feel one another even when they are tens of microns apart. Furthermore, the speed of approach was not constant. Rather, it diverged as the ellipsoids approached one another. These features were very reproducible and agree with expectations for capillary interactions. In the inset of Fig. 2, we plot $r(t_{\max} - t)$ on a log-log scale. $t_{\max}$ corresponds to the time when the particles come into contact. Interestingly, the long-time data were well fit by the power law,

$$r = (t_{\max} - t)^{\alpha}, \tag{1}$$

with $0 < \alpha < 1$. This behavior holds for both tip-to-tip and side-to-side interactions.

The pair interaction potential can be derived from the equation of motion for the ellipsoid and some reasonable approximations. The equation of motion for an ellipsoid of mass m is: $md^2\mathbf{r}/dt^2 = \mathbf{F}_{\text{drag}} + \mathbf{F}_{\text{inter}} + \mathbf{F}_{\text{stoch}}$. $\mathbf{F}_{\text{stoch}}$ is the stochastic thermal force, $\mathbf{F}_{\text{drag}}$ the viscous drag force, and $\mathbf{F}_{\text{inter}}$ the sought after interaction force. We neglect $\mathbf{F}_{\text{stoch}}$ compared to the other terms because the fluctuations are

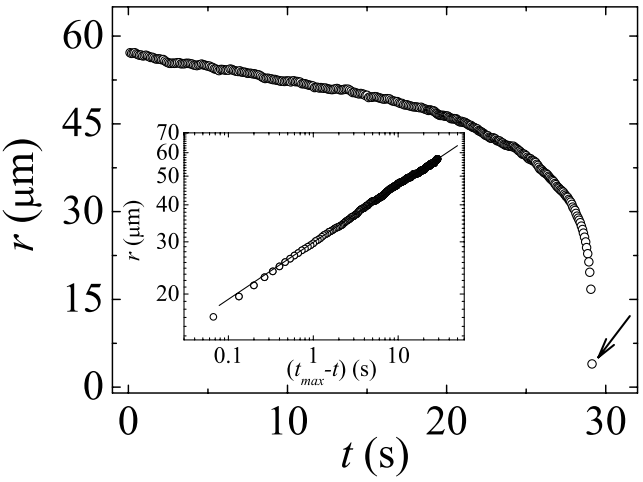

FIG. 2. Center-to-center separation distance, r, as a function of time t extracted from image analysis. The arrow indicates when the ellipsoids make contact and provides $t_{\max}$. Inset: log$r$ vs log$(t_{\max} - t)$ illustrating the power law from Eq. (1).

very weak. Taking typical maxima of the velocity and acceleration, the inertial term is of order $10^{-15}N$. For ellipsoidal particles, the drag force depends on the relative orientation of the ellipsoid with respect to the translating velocity $\mathbf{v}$. We used the following extended form of the Stokes formula to compute the drag force [22]: $\mathbf{F}_{\text{drag}} = -\eta\tilde{c}\mathbf{v}$ with $\tilde{c} = \sqrt{c_a^2\cos^2\theta + c_c^2\sin^2\theta}$. θ is the angle between the long axis of the ellipsoid and the velocity $\mathbf{v}$. Here c (a) denotes the semilong (semishort) axis, η is the viscosity of the liquid (matched for the oil and water phases), c_a and c_c are drag resistance coefficients which depend on a, c, and $k = c/a$ (see [22]). Taking typical experimental values, $\eta = 0.1$ Pa. s, $\tilde{c} \approx 60\ \mu$m, and $v_{\max} \approx 100\ \mu$m/s, we obtain $F_{\text{drag}} \approx 10^{-10}N$. Therefore, the inertial term can be neglected. As a result, at any point of the trajectory, the drag force is equal in magnitude to the interaction force: $\mathbf{F}_{\text{drag}} = -\mathbf{F}_{\text{inter}}$. A spatial integration along the trajectory recovers the pair interaction potential $U(r)$: $U(r) = -\eta\tilde{c}\int_{r_{\text{contact}}}^{r} v(r')dr'$ where r_{contact} is the distance between the centers of mass at contact.

The Stokes formula employed above is valid in bulk fluids. According to Danov *et al.* [23], an error of 10%–20% is made when the "bulk" formula is used to describe the Stokes drag of spheres adsorbed at a liquid-gas interface. Our analysis is therefore approximate, but since we are primarily interested in the order of magnitude, the effect is of minor importance to our conclusions.

The above considerations and Eq. (1) imply that the measured pair interaction potential should scale as

$$U(r) \propto r^{\beta}, \tag{2}$$

with $\beta = 2 - 1/\alpha < 0$. Figure 3 shows a representative plot of $U(r)$ in units of k_BT, deduced from an experimental $r(t)$ curve. The inset illustrates the power law behavior suggested by Eq. (2). Experimental values of β are reported in Table I. Tip-to-tip and side-to-side approaches were observed for both PS and Si ellipsoids (after contact, the Si ellipsoids typically realigned to form side-to-side chains). Close to contact, the measured capillary attraction was several orders of magnitude greater than k_BT, with typical values greater than $10^5 k_BT$ for Si ellipsoids (see Table I). These numbers are within 1 order of magnitude of theoretical estimates for spheres, which predict energies at contact of $(10^3$–$10^4)k_BT$ [9–11]. Tip-to-tip potential measurements for both kinds of ellipsoids were comparable to their side-to-side counterparts.

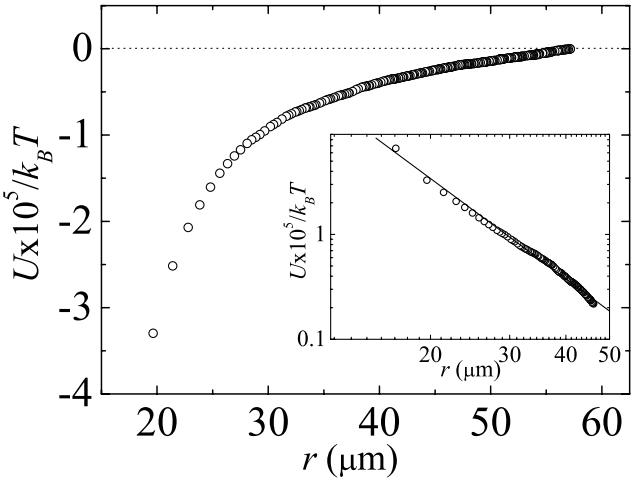

FIG. 3. Pair interaction potential derived from the data in Fig. 2. Inset: log-log plot showing the power law of Eq. (2).

Clearly, the wetting profiles on the particle surfaces control the range and strength of the resulting capillary interactions. Unfortunately, the experimental wetting profiles around single particles are difficult to probe. Nevertheless, the prolate ellipsoidal symmetry suggests, as a first approximation, a profile of quadrupolar symmetry. We have therefore calculated the expected interfacial shape around an ellipsoidal particle in the absence of gravity, which can be neglected here [9,16], and for the special case where we impose a constant contact angle, γ_c, all along the contour (see Fig. 4). Under such conditions, the solution is known for spheres: the interface is planar and satisfies the Young relation [24]. The result, however, is different for ellipsoids. Assuming small interface slopes and an appropriate set of boundary conditions, the Laplace equation for the interface height $h(r, \theta)$ (using polar coordinates), can be solved analytically to yield

$$h(r, \theta) = \frac{c_0}{2} + \sum_{n=1}^{\infty} c_n \left[\frac{r_c(\theta)}{r}\right]^{2n} \cos(2n\theta), \tag{3}$$

where c_0 and c_n are known Fourier coefficients, while $r_c(\theta)$ is the contact radius. Figure 4 shows a surface plot of Eq. (3). It can be seen that the interfacial deformations have a quadrupolar symmetry with h lower along the long-axis direction than along the short-axis one. Thus, it is reasonable to expect that prolate ellipsoidal particles trapped at a fluid interface should behave as capillary quadrupoles and interact as such. Interestingly, spherical capillary quadrupoles are predicted to interact at long range according to a power law with r^{-4} dependence [9–11]. This behavior is similar to our experiments and it is tempting, as a first approximation, to describe the trapped ellipsoids as capillary quadrupoles.

TABLE I. Contact energies, U_{contact}, for the two kinds of ellipsoids. The exponent β is also reported for two geometries of approach, with $3 \leq k \leq 4.3$.

	PS Ellipsoids	Si Ellipsoids
U_{contact} (k_BT)	$\sim 10^4$	$>10^5$
β (PS and Si)	tip-tip: -4 ± 0.3	
	side-side: -3.1 ± 0.2	

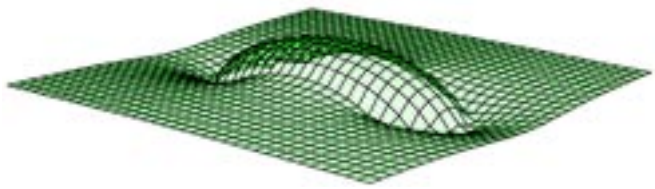

FIG. 4 (color online). Possible interfacial profile around an ellipsoidal particle. The deformations have a quadrupolar symmetry.

In summary, we have discovered that micron-sized ellipsoidal particles trapped at a fluid-fluid interface interact through strong, long-ranged capillary attractions which largely exceed k_BT. These attractions lead to the formation of open branched aggregates with a clear tendency towards chaining. The power law behavior of the pair interaction potential is roughly consistent with a description in terms of capillary quadrupoles. Spheres with the same surface chemistry behave differently, highlighting the importance of particle shape in capillary interactions. For the future, it is desirable to probe interfacial deformations directly, and explore the role of aspect ratio quantitatively.

We thank M. Nobili, M. F. Islam, Z. Dogic, D. T. Chen, M. Bryning, B. Pouligny, R. Kamien, and T. C. Lubensky for helpful discussions. This work was supported by the NSF through Grants No. DMR-0203378 and the PENN MRSEC No. DMR-00-79909.

[1] B. P. Binks, Curr. Opin. Colloid Interface Sci. **7**, 21 (2002) and references therein.
[2] K. Zahn and G. Maret, Phys. Rev. Lett. **85**, 3656 (2000).
[3] T. S. Horozov, R. Aveyard, J. H. Clint, and B. P. Binks, Langmuir **19**, 2822 (2003) and references therein.
[4] A. R. Bausch *et al.*, Science **299**, 1716 (2003).
[5] P. A. Kralchevsky and K. Nagayama, Adv. Colloid Interface Sci. **85**, 145 (2000).
[6] P. A. Kralchevsky and N. D. Denkov, Curr. Opin. Colloid Interface Sci. **6**, 383 (2001).
[7] K. D. Danov, P. A. Kralchevsky, and M. P. Boneva, Langmuir **20**, 6139 (2004).
[8] M. G. Nikolaides *et al.*, Nature (London) **420**, 299 (2002).
[9] D. Stamou, C. Duschl, and D. Johannsmann, Phys. Rev. E **62**, 5263 (2000).
[10] P. A. Kralchevsky, N. D. Denkov, and K. Danov, Langmuir **17**, 7694 (2001).
[11] J. B. Fournier and P. Galatola, Phys. Rev. E **65**, 031601 (2002).
[12] P. Pieranski, Phys. Rev. Lett. **45**, 569 (1980).
[13] R. Aveyard *et al.*, Phys. Rev. Lett. **88**, 246102 (2002).
[14] R. Aveyard, J. H. Clint, D. Nees, and V. N. Paunov, Langmuir **16**, 1969 (2000).
[15] N. Bowden, F. Arias, T. Deng, and G. M. Whitesides, Langmuir **17**, 1757 (2001).
[16] A. B. D. Brown, C. G. Smith, and A. R. Rennie, Phys. Rev. E **62**, 951 (2000).
[17] C. C. Ho, A. Keller, J. A. Odell, and R. H. Ottewill, Colloid Polym. Sci. **271**, 469 (1993).
[18] Y. Hotta, P. C. A. Alberius, and L. Bergström, J. Mater. Chem. **13**, 496 (2003).
[19] ProSciTech, http://www.proscitech.com.au.
[20] J. N. Israelachvili, in *Intermolecular and Surface Forces* (Academic, London, 1992), 2nd ed.
[21] J. C. Crocker and D. G. Grier, J. Colloid Interface Sci. **179**, 298 (1996).
[22] J. Happel and H. Brenner, in *Low Reynolds Number Hydrodynamics* (Klüwer, Dordrecht, 1991).
[23] K. Danov, R. Aust, F. Durst, and U. Lange, J. Colloid Interface Sci. **175**, 36 (1995).
[24] S. A. Safran, in *Statistical Thermodynamics of Surfaces, Interfaces, and Membranes* (Addison-Wesley, Reading, MA, 1994).